EPJ Web of Conferences **106**, 04008 (2016)
DOI: 10.1051/epjconf/201610604008

Photonuclear Studies for the Isomeric Yield Ratios in the Production of $^{nat}Fe(\gamma,xnp)^{52m,g}Mn$ with 50-,60-, and 70-MeV Bremsstrahlung

Md. Shakilur Rahman[1,a], Guinyun Kim[2], Kyung-Sook Kim[2], Manwoo Lee[2], and A.K.M. Moinul Haque Meaze[3]

[1] Institute of Nuclear Science & Technology, Atomic Energy Research Establishment, Bangladesh Atomic Energy Commission, Ganakbari, Savar, Dhaka 1349, Bangladesh
[2] Department of Physics, Kyungpook National University, 1370 Sankyuk-dong, Buk-gu, Daegu 702-701, Republic of Korea
[3] Department of Physics, University of Chittagong, Chittagong 4331, Bangladesh

Abstract. The isomeric yield ratios in the production of $^{nat}Fe(\gamma,xnp)^{52m,g}Mn$ have been measured with photonuclear reactions. The high purity natural Fe metallic foils were used and irradiated with bremsstrahlung beams of end point energy 50-, 60-, and 70-MeV. The bremsstrahlung beams are produced with high energy electron beam struck with 0.1 mm thin tungsten target. The activation method has been used and hence the induced activities in the irradiated foils were measured by off-line γ-ray spectrometric technique using HPGe detector coupled to a PC-based 4K MCA. The experimental values of isomeric ratios are compared with the theoretical values by statistical model code TALYS. The detail of the formation of isomers by photonuclear reactions together with the literature values of the investigated nuclides are compared and discussed.

1. Introduction

Investigation of the properties of excited nuclear states of a nuclear reaction gives the information on the probability of excitation, the energy, and spin distributions. In a nuclear reaction, the relative population of isomeric state and unstable ground state of a nucleus is termed as the isomeric ratio (IR), which can be expressed as σ_m/σ_g, where σ_m and σ_g are the cross-sections for production of isomeric and unstable ground states. Since the isomeric and the ground state differ in spins, the isomeric ratio can also be represented as a ratio of cross-sections for the production of high to low spin state, i.e., $IR = \sigma_{high-spin}/\sigma_{low-spin}$ [1–3]. In case of bremsstrahlung photon irradiation, due to the continuity of the photon energy spectrum, the IR can be represented through the yields of two states, i.e., $IR \equiv Y_{high-spin}/Y_{low-spin}$. This ratio depends on the spin of the target nucleus, and the intake angular momentum determined by the mass and the energy of projectile particles. In simple terms, it is dependent on the distributions of angular momenta in various stages of the reaction.

[a] Corresponding author: shakilknu.kor@gmail.com

During the last few years, the study of isomeric yield ratios has become an important approach for studying the angular momentum effects in nuclear reactions, spin dependence of the nuclear level density, refinements in gamma transition theories and testing of theoretical nuclear models [4–17]. During the last few years the essential progress is observable in the development of new and upgrading existing theoretical models for the reactions considered in this energy region. Some new pre-equilibrium model has been developed in defining multi-particle emission [18, 19] and quasi-deuteron model is enhanced [20]. The rapidly growing interest of Accelerator Driven Subcritical System (ADSS) is in progress and photonuclear data become an important source of information in designing such reactor.

In the present study, the measurements of isomeric ratios of ^{52m,g}Mn production via photonuclear reactions on ^{nat}Fe targets are reported. The present measurement is aimed for the bremsstrahlung energy region 50- to 70-MeV with a step of $\Delta E = 10$ MeV. Natural Fe is extensively used as iron alloy which is the most common structural material of nuclear facilities. The development of high quality nuclear data for iron is practically important mainly due to iron's role as an important structural material in accelerator and ADSS reactor designs. There are number of investigations of isomeric yield ratio of ^{52m,g}Mn production by many authors [16, 21–24] using photonuclear reactions. The yield ratio of this isomer is measured by Kato et al. [21] at 30-MeV bremsstrahlung energy, W.B. Walters et al. [16] in the wide range of bremsstrahlung energy 100- to 250-MeV, Henry et al. [22] at 70-MeV bremsstrahlung, Van Do et al. [23] at 65-MeV bremsstrahlung, and by Kumbartzki et al. [24] at 1500-MeV bremsstrahlung.

The main aim of the present work is to extend our measurement of IRs in the range 50-, to 70-MeV bremsstrahlung with a step of $\Delta E = 10$ MeV by photoactivation method. The experiment is performed with the electron linear accelerator at Pohang Accelerator Laboratory (PAL).

2. Experimental Procedure

2.1 Bremsstrahlung Production

The bremsstrahlung beam of end point energy 50-, 60-, and 70-MeV were produced from 100-MeV electron linac at PAL. The details of the electron linac and bremsstrahlung production are described elsewhere [25, 26]. The accelerator can be operated with the high current accelerating section that can provide high intensity electron beam current with a peak value of 20A. The electron beam was deflected 90° from the original beam path of the accelerating section, and again deflected 45° into the beam exit window. The spread of electron energies in this operating condition was less than 1% from the selected value. The bremsstrahlung photons were produced when a pulsed electron beam hit a 0.1-mm thick W-target with a size of 100 mm × 100 mm. The W-target is located at 18 cm from the beam exit window.

The simulated bremsstrahlung photons generated by electrons with 50-, 60-, and 70-MeV with GEANT4 code [27] is given in [28].

2.2 Sample Irradiation

High-purity natural Fe foils in disc shape, made by the Reactor Experiments Inc. (USA) were exposed to uncollimated bremsstrahlung photons of 50-, 60-, and 70-MeV form the electron linac of the PAL. The characteristics of the samples are given in Table 1. Thin activation foils were used in this experiment, which leads to a strongly reduced or negligible effect of self-absorption of the measured γ-line. The activation foils were placed in air at 12 cm from the W target and they were positioned at zero degree with the direction of the electron beam. During the sample irradiation, the electron linac was operated with a repetition rate of 15 Hz, a pulse width of 1.0 μs, and the average beam current of 23 ± 3 mA, 34 ± 3 mA, and 40 ± 2 mA for 50-, 60-, and 70-MeV, respectively.

Table 1. Characteristics of ^{nat}Fe activation samples.

Sample	Bremsstrahlung energy	Purity (%)	Diameter (cm)	Thickness (cm)	Weight (g)
^{nat}Fe	50 MeV	99.50	1.400±0.008	0.010	0.1220±0.0002
^{nat}Fe	60 MeV	99.50	1.411±0.007	0.010	0.1228±0.0001
^{nat}Fe	70 MeV	99.50	1.410±0.005	0.010	0.1227±0.0001

2.3 Gamma-ray Spectrometry

The detection system consists of a p-type coaxial CANBERRA high-purity germanium (HPGe) detector with a diameter of 60.5 mm and length of 31 mm. The HPGe is connected with multichannel analyzer (MCA) system which is operated with GENIE2000 data acquisition software. The energy resolution of the detector was 1.80 keV full width at half maximum (FWHM) at the 1332.5 keV peak of ^{60}Co. The detection efficiency was 20% at 1332.5 keV relative to a 7.62 cm diameter ×7.62 cm length NaI(Tl) detector. The photo-peak efficiency is calculated with simple relationship [29] with a set of gamma ray standard sources: ^{241}Am and ^{152}Eu. To the crude approximation, the efficiency is inversely proportional to the power of the γ-ray energy by the relationship given in [29]. The measured detection efficiencies were fitted by using the following 5th order polynomial fitting function:

$$\ln \varepsilon = \sum_{n=0}^{5} a_n \left(\ln \left(E/E_0\right)\right)^n . \tag{1}$$

Where, ε is the detection efficiency, a_n represents the fitting parameters, and E is the energy of the photopeak, and E_0 is an arbitrary energy which is set as $E_0 = 1$ keV. The detector efficiencies were measured at different distances between the standard gamma sources and the surface of the detector, ranging from 5 mm to 105 mm in steps of 5 mm. The details of the detector full energy photo-peak efficiency measurement as a function of photon energy are given in [28].

2.4 Radioactivity Measurements

The radioactivity measurement was commenced after the irradiation with an appropriate cooling or waiting time.

The induced gamma activities emitted from the activation foils were measured by using the gamma spectrometer without any chemical purification. The waiting time and the measuring time were chosen based on the activity and the half-life of each radionuclide. In order to optimize the dead-time and the coincidence summing effect we have also chosen the appropriate distance between the sample and the detector for each measurement. Generally, the dead-time was kept below 1.5% during the measurement. Each sample was counted several times in order to obtain decay curves for the photopeaks as well as to observe the linearity of the experimental IR. The number of counts taken and the span of time covered varied from one sample to another but typically 5 or more measurements were made on each sample over about three half-lives of the longest lived component of interest. A typical γ-ray spectra from the investigated foil of ^{nat}Fe irradiated by bremsstrahlung beam of end-point energy 70-MeV is shown in Fig. 1.

3. Activation Data Analysis

3.1 Basic Equations for Isomeric Yield Ratios

In a nuclear reaction, the yield produced in an isomeric-state to that of ground-state is called the isomeric cross-section ratio. In case of the bremsstrahlung photon irradiation, due to the continuity of the energy

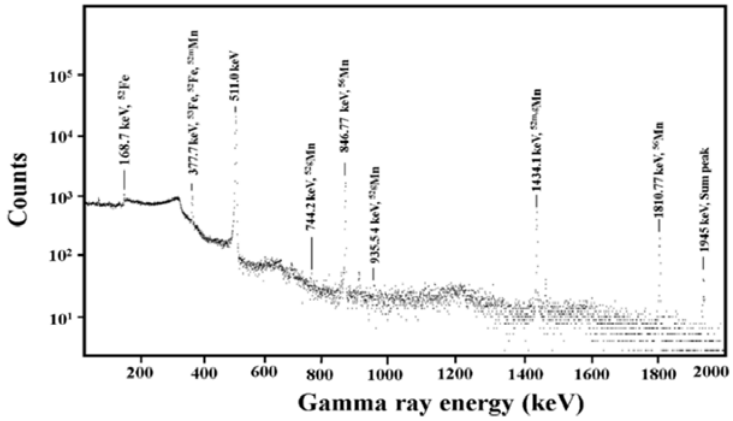

Figure 1. Typical γ-ray spectrum from the activated sample ^{nat}Fe with bremsstrahlung end point energy 70-MeV at an Irradiation time (t_i) = 3 h 01 min, Waiting time (t_w) = 26 min 54 s, and Counting time (t_c) = 16 min 40 s.

spectrum, the isomeric cross-section ratio can also be represented through the yields of the two states instead of two cross-sections which can be expressed as follows:

$$Y_i = N_0 \int_{E_{th}}^{E_{\gamma max}} \sigma_i(E)\phi(E)dE, \tag{2}$$

where i represents the isomeric state (m) or ground state (g) of a isomeric pair product of interest, N_0 is the number of target nuclei, $\sigma_i(E)$ is the energy dependent reaction cross-section and $\phi(E)$ is the shape of the bremsstrahlung spectrum. $E_{\gamma max}$ and E_{th} are the maximum bremsstrahlung energy and the reaction threshold, respectively.

The activities of the reaction product can be determined from the respective photopeak area and detection efficiency. As the pulsed nature of irradiation source is used, the relationship between the γ-rays, activity S_A, and the reaction cross-section can be expressed as follows:

$$S_A = \frac{I_\gamma \varepsilon N_0 K}{\lambda(1-e^{-\lambda T})}(1-e^{-\lambda\tau})(1-e^{-\lambda t_i})e^{-\lambda t_w}(1-e^{-\lambda t_c}) \int_{E_{th}}^{E_{\gamma\,\max}} \phi(E)\sigma(E)dE, \tag{3}$$

where N_0 is the number of target nuclei, ϕ is the incident photon flux, ε is the detection efficiency for the measured γ-ray, K the correction factor for coincidence summing, γ-ray self-absorption, I_γ is the intensity of the γ-ray, λ is the decay constant of the isotope of interest ($\lambda = ln2/T_{1/2}$), τ is the pulse width, t_i is the irradiation time, t_w is the waiting time, t_c is the counting time, T is the cycle period, and $E_{\gamma max}$ and E_{th} are the maximum bremsstrahlung energy and the reaction threshold.

In activation process, considering the production of nuclide of isomeric state and ground state at the same time of irradiation and internal transfer, we can derive the isomeric ratio IR from the measured gamma activities as follows:

$$IR \equiv \frac{Y_g}{Y_m} = \left[\frac{\lambda_g F_m}{\lambda_m F_g} \times \left(K_F \frac{S_g}{S_m} \times \frac{\varepsilon_m I_{\gamma m}}{\varepsilon_g I_{\gamma g}} - \frac{P\lambda_g}{\lambda_g - \lambda_m}\right) + \frac{P\lambda_m}{\lambda_g - \lambda_m}\right] \tag{4}$$

where Y_m and Y_g represent the yields produced in the isomeric and ground states, S_m and S_g are the photopeak areas for the detected γ-rays of the isomeric and the ground state, ε_i is the detection efficiency for the γ-ray of interest, I_γ is the intensity of the γ-ray, P is the branching ratio for the decay of metastable

Table 2. Nuclear reactions and decay data for investigated nuclei ^{52m,g}Mn [30].

Nuclear reaction	Threshold energy, E_{th} (MeV)	Half-life, $T_{1/2}$	Spin states, J^{π}	γ-ray energy, E_γ (keV)	γ-ray intensity, I_γ (%)
^{nat}Fe(γ,xn1p)^{52g}Mn	40.32	21.1 m	6^+	744.23*	90.0
				935.54	94.5
				1246.28	4.21
				1333.65	5.07
				1434.07	100
^{nat}Fe(γ,xn1p)^{52m}Mn	40.70	5.591 d	2^+	377.75	1.7
				1434.07*	98.3
				1727.53	0.22

* γ-rays used in calculations.

to ground state, λ_k is the decay constant of the $k(= m, g)$ state ($\lambda = \ln 2/T_{1/2}$, where $T_{1/2}$ is the half-life of the radioactive isotope), K_F is correction factor accounts for miscounts of photopeak counts due to coincidence summing and self-absorption, and the factor F_k is related as;

$$F_{k=m,g} = \frac{(1 - e^{-\lambda_k \tau}) \times (1 - e^{-\lambda_k t_i}) \times e^{-\lambda_k t_w} \times (1 - e^{-\lambda_k t_c})}{1 - e^{-\lambda_k T}} e^{-\lambda_k (T-\tau)}.$$

3.2 Determination of Isomeric Yield Ratio

The well-known photoactivation method have been used to determine the isomeric yield ratios for the reactions ^{nat}Fe(γ,xnp)^{52m,g}Mn. The produced radionuclides ^{52m,g}Mn were identified based on their characteristic γ-ray energies and half-lives. The decay data of the investigated isomeric pairs were taken from the table of radioactive isotopes are given in Table 2 [30]. The isomeric yield ratios were calculated from the measured activities of the high-spin state to low-spin state of the produced radioisotope.

3.3 Theoretical Calculation by Model Code: TALYS

The theoretical calculation of isomeric yield ratios has been made with statistical model code TALYS [31]. In TALYS, the main contribution in the cross-sections of population both of the isomeric and the ground states gives a statistical mechanism of the nuclear reactions for all energies of γ-rays. Each evaporation step is treated in the framework of the statistical model, taking into consideration the angular momentum and parity conservation, as well as the preequilibrium decay in the neutron emission. TALYS has been compiled and 50 of the discrete low levels are allowed for the automatic regime. The spectroscopic characteristics of nuclear levels, nuclei and decay data are taken from RIPL-2 [32]. Calculating with TALYS, we used Back-shifted Fermi gas Model (BFM) for describing the level density in the continuum energy region. The parameters a – the level density parameter, and δ – the odd-even effects are used as default values. The IR values are calculated for the various energies that modeled from threshold to $E_{\gamma\ max}$ with the step of 1 MeV.

As high-purity iron foil with a natural isotopic composition (^{54}Fe 5.8%, ^{56}Fe 91.72%, ^{57}Fe 2.2%, and ^{58}Fe 0.28%) was used as the target for the irradiation, the ^{52}Mn isomeric pairs could be produced from several reactions, i.e., ^{54}Fe(γ,np)^{52}Mn, ^{56}Fe(γ,3np)^{52}Mn, ^{57}Fe(γ,4np)^{52}Mn, and ^{58}Fe(γ,5np)^{52}Mn reactions for the ^{52}Mn isomer pair. In order to understand the most probable reaction in producing the ^{52m,g}Mn isomeric pairs, we have calculated the reaction yield for each reaction by using Eq. (2), where the reaction cross-section $\sigma_i(E)$ was calculated by using the TALYS code and the bremsstrahlung photon spectrum $\phi(E)$ was obtained from [28]. The reaction yield of the produced ^{52m}Mn and ^{52g}Mn

Table 3. Calculated normalized yield contribution in the production of ^{52m,g}Mn from ^{nat}Fe sample.

Nuclear reaction		Threshold energy, E_{th} (MeV)	Normalized yield contribution, Y_i^N *		
			50 MeV	60 MeV	70 MeV
^{nat}Fe(γ,xnp)^{52m,g}Mn	^{54}Fe(γ,np)^{52m,g}Mn	11.97	91.34×10^{-2}	75.41×10^{-2}	57.88×10^{-2}
	^{56}Fe(γ,3np)^{52m,g}Mn	19.16	8.66×10^{-2}	24.59×10^{-2}	42.12×10^{-2}

* $Y_i^N = \int_{E_{th}}^{E_{\gamma max}} C_i \cdot \sigma_i(E)\phi(E)dE \Big/ \sum_{i=1}^{n} \int_{E_{th}}^{E_{\gamma max}} C_i \cdot \sigma_i(E)\phi(E)dE$, where C_i is the natural composition of isotope in i-th nuclear reaction.

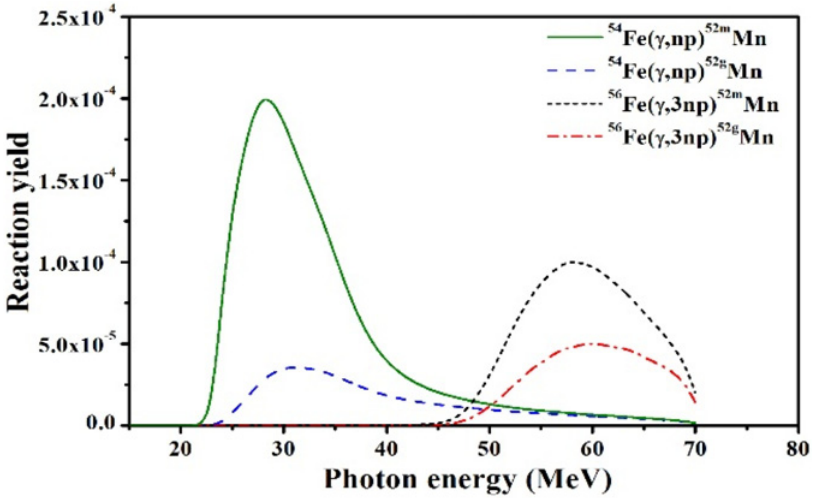

Figure 2. Calculated reaction yields in producing ^{52m}Mn, and ^{52g}Mn isomers from ^{nat}Fe via (γ,n) and (γ,3np) reactions in case of $E_{\gamma max} = 70$ MeV.

formed via (γ,np) and (γ,3np) reactions from natural Fe is shown in Table 3. It is mentioned here that the contribution in forming ^{52m,g}Mn via (γ,4np), and (γ,5np) reaction is negligible due to large reaction threshold and low isotopic abundance in natural composition. The calculated yields for the production of the isomeric pair of ^{52m,g}Mn in case of $E_{\gamma max} = 70$ MeV are shown in Fig. 2.

3.4 ^{nat}Fe(γ, xnp)^{52m,g}Mn

The yield ratios of the isomeric pair ^{52m,g}Mn was determined from the measured activities of isomeric to ground state. According to decay scheme in Fig. 3, the isomeric state, ^{52m}Mn (spin 2$^+$), with a half-life of 21.1 min decays directly to the 1434.07 keV level (2$^+$) of ^{52}Cr by both β^+ and EC processes with a branching ratio of 98.0%. On the other hand, only 1.75% of the isomeric state decays to the unstable ground state, ^{52g}Mn (spin 6$^+$), by emitting the 377.7 keV γ-ray. The unstable ground state, ^{52g}Mn (spin 6$^+$), with a half-life of 5.59 d decays to the 3615.9 keV level (5$^+$) of ^{52}Cr by EC process with a branching ratio of 7.69%, and also to the 3113.9 keV level (6$^+$) of ^{52}Cr by both β^+ and EC processes with a branching ratio of 91.4%. By considering the γ-ray intensity and energy as well as the possible interferences, the activity of the ^{52m}Mn isomeric state was determined based on the 1434.1 keV γ-peak. The main fact of not using the photopeak 377.7 keV is due to its low intensity (1.68%) together with interference of the same γ-peak from ^{52}Fe isotope formed via the ^{nat}Fe(γ,xn)^{52}Fe reactions. In the

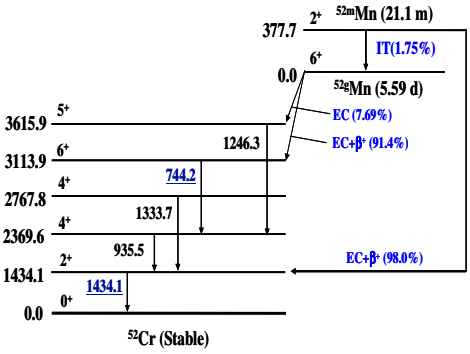

Figure 3. Simplified representation of decay scheme of the isomeric pair ^{52m,g}Mn. The nuclear level energies are in keV.

present data analysis for the ground state activity measurement the photopeak 744.23 keV was used. From the decay scheme, we can see that 744.23 keV γ-peak is interference free, but the 1434.07 keV γ-peak is the mixture of the ^{52m}Mn and ^{52g}Mn. So while determining the activity of the ^{52m}Mn isotope (based on the 1434.1 keV γ-peak) the contribution from the ^{52g}Mn should be subtracted. It is seen that the half life of metastable state (21.1 m) is too small compared to the half life of ground state (5.591 d). So the activity contribution of 1434.07 keV γ-peak due to ^{52g}Mn can be obtained by general decay equation between two consecutive measurements or by analyzing the decay curve.

The natural iron consists of isotopes ^{54,56,57,58}Fe. During the irradiation of natural iron with bremsstrahlung the radioactive isotope ^{52}Fe can be formed via different reaction channels as follows: ^{54}Fe(γ,2n), ^{56}Fe(γ,4n), ^{57}Fe(γ,5n) and ^{58}Fe(γ,6n) with threshold energies of 24.07 MeV, 44.58 MeV, 52.23 MeV and 62.28 MeV, respectively. The ^{52}Fe (with $T_{1/2} = 8.275$ h and the main gamma-ray energy of 168.68 keV (99.2%) decays directly to ^{52}Mn. So, in the activity measurement of ^{52m}Mn, the contribution from the ^{52}Fe was also taken into account. The true coincidence summing effect leads to decrease (summing-out) net photopeak areas of 744.23 keV, and 168.7 keV. The cascading γ-rays are such as: (1) the 744.23 keV and 935.54 keV γ-rays of the ^{52g}Mn, and (2) the 168.69 keV and 377.74 keV of the ^{52}Fe. The summing correction factors due to the cascading gamma rays are calculated based on the measured total and absolute photopeak efficiency curves and the formulae for complex decay schemes given in [33, 34], and it was 1.20 ± 0.03.

The data acquisition and analysis have been performed with Genie 2000 software. The automatic photo-peak search method in Genie 2000 give different threshold peak search option that satisfy up to 95% confidence level. The error the peak area in Genie 2000 is based on non-linear least square technique [35]. The Labsocs codes are used for the error determination. The net peak areas counts are associated with respective uncertainties.

4. Results and Discussion

The yield ratios of ^{52m,g}Mn have been measured from photonuclear reactions are induced by the bremsstrahlung beams of end point energy of 50-, 60-, and 70-MeV. The measured values of isomeric yield ratio together with previous works found in the literature [16, 21–24] for wide energy range are summarized in Table 4. The total uncertainty in Table 4 consists of the uncertainties related to the IR measurement and the systematic uncertainties, which is summarized in Table 5. The uncertainties related to IR measurement were calculated from Eq. (4) by using the error propagation principle based on the uncertainties listed in Table 5. The values of error of half-lives and branching ratios in uncertainty

Table 4. Isomeric yield ratios of ^{52m,g}Mn via (γ,xnp) reactions measured with ^{nat}Fe target.

Nuclear Reaction	Photon energy in MeV	IR= $Y_{high\text{-}spin}/Y_{low\text{-}spin}$		
		Present work	References	Theoretical value by TALYS
^{nat}Fe(γ,xnp)^{52m,g}Mn	30	-	0.102 [21]	-
	50	0.26±0.04	-	0.23
	60	0.32±0.04	-	0.29
	65	-	0.28±0.04 [23]	-
	70	0.33±0.03	0.32±0.05 [22]	0.35
	100	-	0.39±0.03 [16]	-
	150	-	0.36±0.02 [16]	-
	200	-	0.35±0.02 [16]	-
	250	-	0.37±0.02 [16]	-
	1500	-	0.87±0.10 [24]	-

Table 5. Uncertainty sources in the isomeric yield ratio measurements.

Source of Uncertainty		Uncertainties (%)		
		50	60	70
Measurement Error	Statistical error	6-17	3-25	2-11
	Detection efficiency	3-4	3-4	3-4
	Half-life	0.9	0.9	0.9
	Branching ratio	2.8	2.8	2.8
Uncertainties related to IR measurement		12.7	9.9	6.0
Systematic Error	Sample to detector position		1-2	
	Photopeak selection		3-4	
	Electron beam energy		~1	
	Coincidence summing		4-5	
	γ-ray self absorption		0.0	
	Irradiation and waiting time		0.5-1	
Uncertainties related to Systematic			6.9	
Total Uncertainties		14.4	12.1	9.1

calculations were taken from Tables of Isotope [30]. The uncertainty listed in Table 5 indicates the maximum uncertainty of the measured values.

The isomeric yield ratios for the ^{nat}Fe(γ,xnp)^{52m,g}Mn reaction was measured for 50-, 60-, and 70-MeV bremsstrahlung beam and is reported as 0.26±0.04, 0.32±0.04 are 0.33±0.03 respectively. The value reported here are the average values of several measurements of the activated foil. The present results together with the existing literature data are summarized in Table 4. The present results are the first measurements at 50-, and 60-MeV. The main sources of the errors are due to uncertainties in net photopeak counts, photopeak efficiency, coincidence summing, half-lives of nuclide, and branching ratio together with systematic error which is given in Table 5. From the Table 4, we can see that the isomeric yield ratio of ^{52}Mn isomer is measured by Kato et al. [21] at 30-MeV bremsstrahlung, W.B. Walters et al. [16] in the wide range of bremsstrahlung energy 100- to 250-MeV. The yield ratio of the same isomer is reported by V.D. Nguyen et al. [23] at 65 MeV bremsstrahlung from natural Fe target which lies in between the present measurement at 60-, and 70-MeV. The present measurement shows an agreement with V.D. Nguyen et al. within the error limit. The isomeric ratio of ^{52m,g}Mn at 70-MeV bremsstrahlung is measured by Henry et al. [22] which is reported as 0.32±0.05. The value

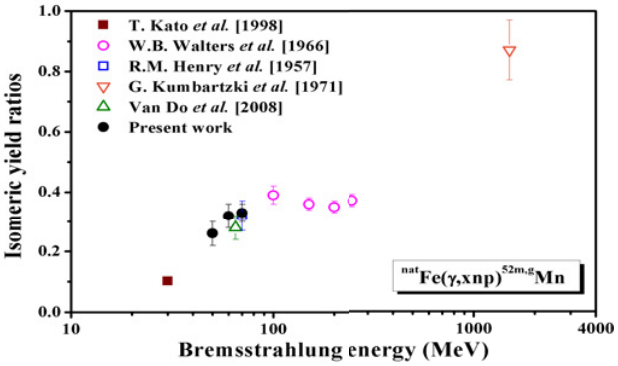

Figure 4. Isomeric yield ratios of ^{52m,g}Mn via photonuclear reaction as a function of end point energy of the incident bremsstrahlung beam.

obtained from the present experiment for the same bremsstrahlung energy is 0.33±0.03 which shows good in agreement with Henry et al. [22] lies within the error limit. However, there are no literature data for direct comparison with the results measured at 50-, and 60-MeV bremsstrahlung energies. The measured isomeric yield ratios together with literature data are plotted in Fig. 4. It is seen that the isomeric yield ratios increase with the increasing bremsstrahlung energies from the threshold up to about 100-MeV. The present measured values shows a good trend with the other values by Kato et al. [21], Henry et al. [22], and Walter et al. [16] which made the measurement authenticated. We have calculated the theoretical values of IR with statistical model code TALYS which is reported in Table 4. The experimental values found a good in agreement with the theoretical values within the error limit. In the present measurement, IR's of ^{52m,g}Mn have been measured from the natural target of Fe which has isotopic composition of ^{54}Fe, ^{56}Fe, ^{57}Fe, and ^{58}Fe. To observe the contributions of ^{54}Fe, and ^{56}Fe in forming ^{52m,g}Mn, we have calculated the reaction weighting coefficients which is shown in Table 3.

5. Conclusion

We have measured the isomeric yield ratios of ^{52m,g}Mn via ^{nat}Fe(γ,xnp)^{52m,g}Mn reaction with the bremsstrahlung end-point energy of 50-, 60-, and 70-MeV. The present result of IR of ^{52m,g}Mn isomer at 70-MeV is very much consistent with the literature values. Two other values of ^{52m,g}Mn at 50-, and 60-MeV bremsstrahlung are the first measurement. We observed that the isomeric yield ratio depends on the incident bremsstrahlung energy for the investigated nuclear reactions. The increasing isomeric ratio indicates the increased transfer of angular momentum in the reaction process. It is also observed that at higher energy the differences of IR values are very small compared to lower energy. This fact can be explained with low momentum transfer in the photonuclear reaction process.

References

[1] R. Volpel, Nucl. Phys. A **182**, 411 (1972)
[2] H. Bartsch, K. Huber, U. Kneissl, H. Krieger, Nucl. Phys. A **256**, 243 (1976)
[3] D. Kolev, E. Dobreva, N. Nenov, V. Todorov, Nucl. Instr. and Meth. A **356**, 390 (1995)
[4] J.R. Huizenga, R. Vandenbosch, Phys. Rev. **120**, 1305 (1960)
[5] R. Vandenbosch, J. R. Huizenga, Phys. Rev. **120**, 1313 (1960)
[6] J. H. Carver, G. E. Coote, T. R. Sherwood, Nucl. Phys. **37**, 449 (1962)
[7] J. L. Need, Phys. Rev. **129**, 1302 (1963)

[8] C.T. Bishop, J. R. Huizenga, and J. P. Hummel, Phys. Rev. **135**, B401 (1964)
[9] C. Riley, K. Ueno, B. Linder, Phys. Rev. **135**, B1340 (1964)
[10] C. T. Bishop, H. K. Vonach, J. R. Huizenga, Nucl. Phys. **60**, 241 (1964)
[11] R. Vandenbosch, L. Haskin, J. C. Norman, Phys. Rev. **137**, B1134 (1965)
[12] I. R. Williams, K.S. Toth, Phys. Rev. **138**, B382 (1965)
[13] N. D. Dudey, T. T. Sugihara, Phys. Rev. **139**, B896 (1965)
[14] J. Bacso, J. Csikai, B. Kardon, D. Kiss, Nucl. Phys. **67**, 443 (1965)
[15] S. Costa, F. Ferrero, S. Ferroni, L. Pasqualini, E. Silva, Nucl. Phys. **72**, 158 (1965)
[16] W. B. Walters and J. P. Hummel, Phys. Rev. **150**, 867 (1966)
[17] I.-G. Birn, B. Strohmaier, H. Freiesleben, S.M. Qaim, Phys. Rev. C **52**, 2546 (1995)
[18] M. Herman, P. Oblozinsky, R. Capote, M. Sin, A. Trkov, A. Ventura, V. Zerkin, International conference of nuclear data for science and technology-ND2004, Melville, AIP Conf. Proc. **769**, 1184 (2005)
[19] P. Talou, T. Kawano, P.G. Young, M.B. Chadwick, Nucl. Instrum. Methods A **562**, 823 (2006)
[20] M.B. Chadwick, P. Oblozinsky, P.E. Hodgson, G. Reffo, Phys. Rev. C **44**, 814 (1991)
[21] T. Kato, Y. Oka (1972), Talanta, **19**, 515 (1972)
[22] R. M. Henry, D. S. Jr. Martin, Phys. Rev. **107**, 772 (1957)
[23] N. Van Do, P. D. Khue, T. T. Kim, T. D. Thiep, V. D. Phung, Y. S. Lee, G. N. Kim, Y. D. Oh, H. S. Lee, H. Kang, M. H. Cho, I. S. Ko, W. Namkung, J. Korean Phys. Soc. **50**, 417 (2007)
[24] G. Kumbartzki, U. Kim, Nucl. Phys. A **176**, 23 (1971)
[25] G. N. Kim et al., J. Korean Phys. Soc. **38**, 14 (2001)
[26] G. N. Kim et al., J. Korean Phys. Soc. **42**, 479 (2003)
[27] S. Giani et al. (GEANT 4 Collaboration), An object-oriented toolkit for simulation in HEP, CERN/LHCC 98-44, (1988). `http://cern.ch/geant4`
[28] M. S. Rahman, K.-S. Kim, M. Lee, G. N. Kim, Y. Oh, H.-S. Lee, M.-H. Cho, I. S. Ko, W. Namkung, N. V. Do, P. D. Khue, K. T. Thanh, T.-I. Ro, Nucl. Instr. Meth. B **267**, 3511 (2009)
[29] G. L. Molnar, Zs. Revay, T. Belgye, Nucl. Instrum. Meth. A **489**, 140 (2002)
[30] R. B. Firestone, C. M. Baglin, F. S. Y. Chu, Table of Isotopes, 8th Edition. Update on CD-ROM. Wiley, New York, (1998)
[31] A. Koning et al., TALYS 1.0, A nuclear reaction program, User manual, (2007). `http://www.talys.eu/download-talys/`
[32] T. Belgya et al.: Handbook for calculations of nuclear reaction data: reference input parameter library, International Atomic Energy Agency. `http://www-nds.iaea.or.at/RIPL-2/`
[33] F. Piton, M. C. Lepy, M. M. Bea, J. Plagnard, Appl. Radiat. Isot. **52**, 791 (2000)
[34] G. J. McCallum, G. E. Coote, Nucl. Instr. and Meth. **130**, 189 (1975)
[35] Customization manual: Genie 2000 spectroscopy system, available in web: <`http://www.canberra.com`>